Enzyme Catalysis

DOI: 10.1002/anie.201204266

Charge-Balanced Metal Fluoride Complexes for Protein Kinase A with Adenosine Diphosphate and Substrate Peptide SP20**

Yi Jin, Matthew J. Cliff, Nicola J. Baxter, Hugh R. W. Dannatt, Andrea M. Hounslow, Matthew W. Bowler, G. Michael Blackburn, and Jonathan P. Waltho**

Phosphoryl transfer reactions underpin multiple roles of phosphate esters and anhydrides in life.[1] Extensive studies on phosphoryl group (PO_3^-) transfer by a wide range of enzymes have made good use of aluminum fluoride complexes as mimics of the transferring PO_3^- ion in transition-state-analog (TSA) structures. The majority are octahedral complexes with square-planar tetrafluoroaluminate ligands.[2] However, they are nonisosteric with the generally accepted trigonal-bipyramidal transition state (TS) for in-line phosphoryl group transfer.[2a,b, 3] More recently, TSA complexes with this geometry, centered around a trifluoromagnesate ligand, have been crystallized for several enzymes, including β-phosphoglucomutase (βPGM),[2c,g] phosphoserine phosphatase (PSP),[2d] phosphoglycerate kinase (PGK),[2h] RhoA/RhoGAP,[4] and a DNA helicase.[5] These MgF_3^- complexes are much closer to being isosteric with the true TS for phosphoryl transfer. Both MgF_3^- and AlF_4^- ligands have the same monoanionic charge as that on the transferring PO_3^- group. In this charge state, the number of positive and negative charges on moieties contributing to the active site is effectively balanced. This is thought to help overcome the inherent repulsion of attack by a nucleophile on the dianionic phosphate residue, described as the anionic shield.[2a]

By contrast, the trigonal aluminum trifluoride moiety (AlF_3^0) has been assigned as the central ligand in over forty trigonal-bipyramidal (tbp) complexes of phosphoryl transfer enzymes. These ligands would be phosphoryl group mimics of net zero charge.[6] However, we established[2d] by ^{19}F NMR spectroscopy that the reported AlF_3^0 ligand in PSP is in reality a MgF_3^- ion, whereas in a charge-depleted variant of PGK we found that, although an AlF_3^0 moiety was present, it was square-planar with water as the fourth ligand.[2h] Thus, identifying tbp metal fluoride moieties is nontrivial. They normally cannot be resolved by protein crystallography alone because there is no difference in electron count between AlF_3^0 and MgF_3^-. Moreover, in structures at lower resolution (≥ 2.8 Å), ligands assigned by convention to be AlF_3^0 cannot be resolved unambiguously from AlF_4^-, as recognized previously.[7] On the other hand, since millimolar fluoride readily leaches aluminum from glass, ligands assigned as MgF_3^- can in reality be AlF_3^0. It is thus imperative that the identity of the metal fluoride moieties should not be trusted unless independently verified by an orthogonal method.[2,4] Critically, knowledge of the exact identity of these metal fluoride complexes is pressing because of the centrality of charge density in mechanistic analysis of enzymes where highly charged nucleotides are substrates.[8]

Where metal fluoride moieties have been unambiguously identified in wild-type phosphoryl transfer enzymes by ^{19}F NMR spectroscopy, they are monoanionic (MgF_3^- or AlF_4^-); that is, charge is prioritized over geometry.[2d,h] These observations have led to a charge balance hypothesis (CBH), which proposes that local charge balance dominates the stabilization of the TS for phosphoryl transfer enzymes.[2a,h] The CBH has been useful as a guiding principle that can identify apparent inconsistencies in interpretation of analytical data and mechanistic analysis for phosphoryl transfer meriting a more thorough analysis. However, all of the data underpinning the CBH are from phosphoryl transfer enzymes that use a single catalytic magnesium ion. The behavior of such enzymes that employ a different number of catalytic magnesium or other ions has not been similarly established.

Protein kinases (PKs)[9] typically use two catalytic magnesium ions[10a] and transfer the γ-phosphate of adenosine triphosphate (ATP) to a hydroxyl group of serine, threonine, or tyrosine residues in target proteins, forming phosphoprotein and adenosine diphosphate (ADP). Hitherto, no protein kinase has been adequately analyzed to define unambiguously its metal fluoride TSA complex, while existing partial information[2i,10] is contradictory. Cyclic adenosine monophosphate (AMP) dependent protein kinase (cAPK) is the archetypal example of some 2000 eukaryotic PKs.[9] Its solution dynamics have been studied extensively[11] but no TSA complex has been fully characterized. We now show that in solution cAPK forms an AlF_4^- (rather than an AlF_3^0) TSA complex with substrate peptides and two catalytic magnesium ions. It thus conforms to the CBH. cAPK also forms an MgF_3^- TSA complex that is fully CBH compatible, and both of these monoanionic metal fluoride species are present in the crystalline state. This selection of unit charge also extends

[*] Dr. Y. Jin, Dr. M. J. Cliff, Dr. N. J. Baxter, Dr. H. R. W. Dannatt, A. M. Hounslow, Prof. Dr. G. M. Blackburn, Prof. Dr. J. P. Waltho
Department of Molecular Biology and Biotechnology
University of Sheffield, Sheffield, S10 2TN (UK)
E-mail: g.m.blackburn@sheffield.ac.uk
j.waltho@sheffield.ac.uk
Dr. N. J. Baxter, Prof. Dr. J. P. Waltho
Manchester Institute of Biotechnology, Manchester, M1 7DN (UK)
Dr. M. W. Bowler
European Molecular Biology Laboratory and
Unit of Virus Host-Cell Interactions
UJF-EMBL-CNRS, UMI 3265, 6 rue Jules Horowitz
BP 181, 38042, Grenoble (France)

[**] The expression construct for cAPK from mouse was provided by Dr. Peter Rellos, SGC, Oxford (UK). We thank the University of Sheffield for a Studentship (to Y.J.) and BBSRC for Grant No. I002146.

Supporting information for this article is available on the WWW under http://dx.doi.org/10.1002/anie.201204266.

to a ground state analog (GSA), as cAPK additionally forms a BeF_3^- complex in solution.

cAPK readily forms a cAPK-ADP-AlF_4^--SP20 TSA complex from its constituent components (see the Supporting Information) where SP20 is a peptide analog of a substrate protein containing the target serine residue at position 17. Four peaks are observed in the ^{19}F NMR spectrum with a 1:1:1:1 ratio of integrals, characteristic of an AlF_4^- TSA species (Figure 1c and Table 1). Chemical shifts for two resonances, F_C and F_D, are at significantly higher field than

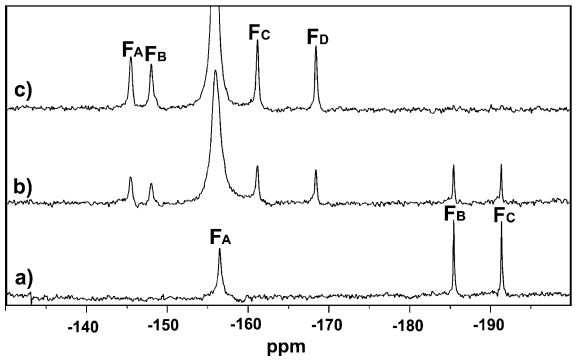

Figure 1. ^{19}F NMR spectra of cAPK-ADP-SP20 metal-fluoride TSA complexes at pH 7.5 and 298 K: a) cAPK-ADP-MgF_3^--SP20 TSA complex, b) after addition of 1.8 mM $AlCl_3$ to the cAPK-ADP-MgF_3^--SP20 TSA complex, and c) after addition of 3.4 mM $AlCl_3$ showing complete conversion into the cAPK-ADP-AlF_4^--SP20 TSA complex.

Table 1: ^{19}F NMR chemical shifts (ppm) of the cAPK-ADP-MgF_3^--SP20 TSA, cAPK-ADP-AlF_4^--SP20 TSA, and cAPK-ADP-BeF_3^--SP20 GSA complexes. The corresponding data for the MEK6-ADP-AlF_4^--p38α TSA complex are provided for comparison.[2i]

Complex	F_A	F_B	F_C	F_D
cAPK-ADP-MgF_3^--SP20	−157[a]	−185	−191	–
cAPK-ADP-AlF_4^--SP20	−146	−148	−161	−168
MEK6-ADP-AlF_4^--p38α	−142	−148	−154	−167
cAPK-ADP-BeF_3^--SP20	−166	−182	−187	–

[a] Signals for MgF^+ ($MgF(H_2O)_5^+$) and F_A coincide but are resolved by 180° inversion of the free F^- signal.

those for enzyme complexes having a single catalytic Mg^{II} ion and their linewidths are narrower than those of F_A and F_B. These data accord with the coordination of F_C and F_D by two catalytic Mg^{II} ions within the TSA complex and with a corresponding reduction in hydrogen-bonding partners.[10a] Such sensitivity of ^{19}F chemical shift to coordination and to hydrogen bonding is well-established.[2g] The AlF_4^- TSA complex does not exchange with free fluoride during a 1 s timeframe (see the Supporting Information).

Following rigorous sequestration of aluminum by deferoxamine, a cAPK-ADP-MgF_3^--SP20 TSA complex assembles in the presence of Mg^{II}, fluoride, ADP, and the synthetic substrate peptide SP20. Its ^{19}F NMR spectrum shows two well-resolved resonances of equal intensity (F_B and F_C, Table 1, Figure 1a and Figure S1a in the Supporting Information). A third resonance, $F_A = -157$ ppm, is partially obscured by the broad peak of free MgF^+, but is revealed in a spectrum derived by summation of a standard spectrum and one in which the MgF^+ resonance is inverted, using a selective 180° pulse applied to the free F^- signal at −119 ppm. This also inverts the MgF^+ resonance through fast exchange (Figure 1a and Figure S1b,c in the Supporting Information).

cAPK also forms a MgF_3^- TSA complex under similar conditions with Kemptide, a synthetic heptapeptide substrate.[12] The ^{19}F chemical shifts of the cAPK-ADP-MgF_3^--Kemptide and the cAPK-ADP-MgF_3^--SP20 TSA complexes are indistinguishable, indicating that the active-site architecture places the fluorine atoms of the trigonal ligand in closely equivalent electronic environments, despite embracing two significantly different peptide substrates (see Figure S2a,b).

All of the metal fluoride TSA solution complexes of cAPK formed with ADP and substrate peptide have monoanionic ligands at their core. There is no evidence for the formation of an AlF_3^0 TSA complex, and thus the behavior of this archetypal PK, with two catalytic Mg^{II} ions,[10a] mirrors that of phosphoryl transfer enzymes using a single catalytic Mg^{II} ion. On increasing the pH above neutrality, the AlF_4^- complex is progressively displaced by the MgF_3^- complex, with the AlF_4^- and MgF_3^- TSA complexes visibly co-existing in the pH range 7.5 to 8.5 (Figure S3). Such a switch from aluminum to magnesium fluoride has been characterized previously for PSP and βPGM,[2d] and arises from the well-established precipitation of aluminum hydroxide in mildly alkaline solutions.[2d,h,13] In the absence of aluminum, the ^{19}F resonances of the MgF_3^- complex remain constant in chemical shift and intensity across the pH range 6.0 to 9.0. This shows that none of the charged groups closely associated with the active site change their protonation state across this pH range in the TSA complex.

In previous studies, such MgF_3^- solution complexes have been correlated with solid-state complexes having tbp geometry, as shown by high-resolution protein crystallography for βPGM,[2g] PGK,[2h] and PSP.[2d] A tbp metal trifluoride TSA complex has been reported for cAPK (protein data bank PDB: 1L3R),[10a] which accords structurally with the MgF_3^- complex observed in solution but was assigned chemically as an AlF_3^0 complex. As the cAPK complex crystals were processed at pH 8.0,[10a] the clear conclusion is that the diffraction data were obtained from a crystal dominated by a trifluoromagnesate complex. That analysis is endorsed by the length of the axial bonds in the tbp crystal complex. Our unrestrained de novo refinement of the cAPK metal fluoride TSA crystal structure against the deposited structure factors (1L3R) shows full agreement with the longer metal–oxygen axial bond lengths associated with MgF_3^- complexes.[2b,c,g,h] The data refine to M–O_{ax} of 2.27 and 2.31 Å (see the Experimental Methods in the Supporting Information), compared to typical values of 2.1 to 2.2 Å in other MgF_3^- complexes and of 1.9 to 2.05 Å in AlF_4^- complexes.[2g] Furthermore, inspection of the electron density difference map ($F_o - F_c$) reveals additional positive density (peak heights 4.5 σ) in two loci contiguous to the core of the tbp moiety. This density (Figure S4) is fully consistent with dual occupancy of the TSA by a major tbp moiety (Figure 2a) and a minor octahedral moiety (Figure 2b). Analysis of atomic *B*-factor

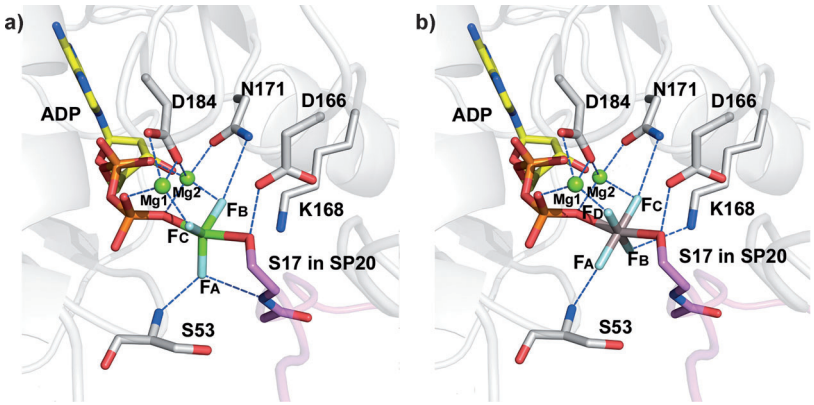

Figure 2. Structure of tbp cAPK-ADP-MgF_3^--SP20 and octahedral cAPK-ADP-AlF_4^--SP20 TSA complexes derived from unrestrained refinement of the deposited diffraction data (protein data base PDB: 1L3R).[10a] a) The AlF_3^0 moiety re-assigned as MgF_3^- with atom numbering F_1, F_2, and F_3 in 1L3R correlating to F_B, F_C, and F_A, respectively, in the ^{19}F NMR spectrum of the MgF_3^- TSA complex. b) The AlF_4^- moiety assigned on the basis of additional positive density in the active site (in 1L3R). Fluorine atoms are identified by ^{19}F NMR chemical shifts and SIIS data.

values is consistent with an active-site occupancy ratio of about 3:1 tbp MgF_3^- to octahedral AlF_4^-.

Solvent-induced isotope shift (SIIS) values are sensitive probes of the coordination environment of fluorine atoms, reporting how well nuclei are coordinated by solvent-exchangeable hydrogen atoms.[14] In conjunction with the TSA complex structures, they enable assignment of the ^{19}F NMR resonances (Table 2 and Figure 2). For the MgF_3^- TSA complex, the SIIS value is largest for F_A (1.4 ppm) showing a high local proton density,[2d] consistent with its downfield chemical shift[2g,h] (Tables 1 and 2). Values for F_B (0.3 ppm) and F_C (0.2 ppm) and their upfield chemical shifts identify their coordination by the catalytic Mg^{II} ions. Hence, F_A corresponds to the fluorine coordinating the amides of Ser53 in cAPK and Ser17 in SP20 (S53 and S17 in Figure 2). A long hydrogen bond (3.1 Å) to the side chain of Asn171 is a likely source of the slightly enhanced SIIS and more downfield chemical shift of F_B relative to F_C (Table 2 and Figure 2a). Similarly, for the AlF_4^- complex, the two upfield resonances correspond to fluorines that coordinate the Mg^{II} ions: F_D with the smaller SIIS is assigned as coordinating to Mg1, with F_C coordinating to Mg2 and the sidechain of Asn171 (Figure 2b). Of two downfield resonances, F_A has the larger SIIS (Table 2) and is assigned as coordinating to Ser53 while F_B coordinates Lys168.

Table 2: Solvent-induced isotope shifts (SIIS, ppm) for the ^{19}F signals of the cAPK-ADP-MgF_3^--SP20 TSA, cAPK-ADP-AlF_4^--SP20 TSA, and cAPK-ADP-BeF_3^--SP20 GSA complexes.

Complex SIIS[a]	F_A	F_B	F_C	F_D
cAPK-ADP-MgF_3^--SP20	1.4	0.3	0.2	–
cAPK-ADP-AlF_4^--SP20	0.8	0.6	0.4	0.1
cAPK-ADP-BeF_3^--SP20	0.8	0.2	0.1	–

[a] SIIS = $\delta^{19}F(H_2O$ buffer$) - \delta^{19}F(D_2O$ buffer$)$.

Analysis of charge in the vicinity of the active site of these TSA complexes fully endorses the adherence of cAPK to the CBH in its TS. For the MgF_3^- complex, the net charge oscillates around the zero charge axis, while for an AlF_3^0 complex net charge is significantly positive out to about 13 Å from the transferring phosphorus atom (Figure 3, black and red curves, respectively). This charge balance is achieved as a result of four cationic residues in the SP20 substrate peptide. The charges of arginines 11, 14, and 15 and histidine 19 are within 12 Å of the transferring phosphorus while the three carboxylate groups are beyond 13.5 Å.

We also observed that cAPK forms a beryllium fluoride cAPK-ADP-BeF_3^--SP20 GSA complex in the presence of Be^{II}, fluoride, ADP, and SP20. Its ^{19}F NMR spectrum shows two well-resolved resonances of equal intensity, F_B and F_C. A third resonance, $F_A = -166$ ppm, is distinguished from those of free BeF_x by its dependence on beryllium concentration (see Figure S5 in the Supporting Information). Its downfield chemical shift identifies it as the fluorine not ligated to either catalytic Mg^{II} ion, and is endorsed by an SIIS (0.8 ppm) consistent with hydrogen-bonding interactions to the amides of Ser17 in SP20 and Ser53 in cAPK. Chemical shift and SIIS values for F_B (0.2 ppm) and F_C (0.1 ppm) identify coordination to the two catalytic Mg^{II} ions, as in the MgF_3^- TSA complex (Tables 1 and 2). No fluoroberyllate complex is observed in the absence of the SP20 peptide, showing that hydrogen bonding to F_A from Ser17 in SP20 is important for complex stabilization and that the complete enzyme–substrate active site is needed to deliver full charge balance for formation of the fluoroberyllate complex (Figure 3, blue curve).

The behavior of two further PKs for which metal fluoride TSA complexes have been reported can now be rationalized. A crystal structure of a tbp TSA complex has been analyzed for CDK2, a serine-threonine PK related to cAPK. It has the enzyme, a substrate peptide, ADP, and a trigonal metal trifluoride, assigned as MgF_3^-, though Al^{III} ions were not

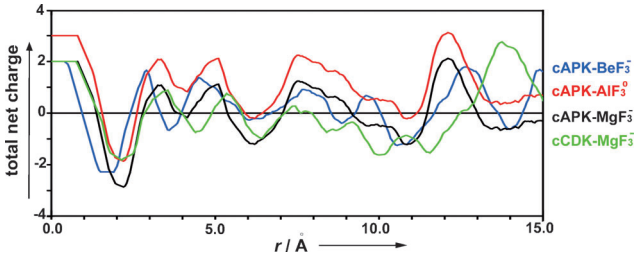

Figure 3. Charge balance calculation for PO_3^- transfer: cAPK with AlF_3^0 (red), CDK2 with MgF_3^- (green), cAPK with MgF_3^- (black), and cAPK with BeF_3^- (blue). The charge is summed over all atoms within a sphere of increasing radius *r*, the center of which is the transferring γ-phosphorus or its magnesium or aluminum surrogate (see the Experimental Methods in the Supporting Information).[2a,h]

rigorously excluded in the formation of the complex,[10b,15] thus a potential AlF_3^0 could not be ruled out. The net charge curve for this complex oscillates around the zero axis and satisfies the CBH (Figure 3, green curve). MEK6 is a PK[2i,16] having a preference for phosphorylation of tyrosine over threonine residues. It forms an AlF_4^- TSA solution complex with ADP and its substrate protein (p38α), shown by ^{19}F NMR spectroscopy, but formation of the equivalent MgF_3^- TSA complex was not observed.[2i] This result means that current TS analysis of these PKs is now unified and the behavior of these classes of enzymes using two catalytic magnesium ions is clearly linked by charge balance to that of the family of single-magnesium phosphoryl transfer enzymes.

A striking novel feature of metal-fluoride TSA complexes for cAPK is the co-existence of AlF_4^- and MgF_3^- complexes in solution, even when the Al^{III} concentration exceeds that of cAPK. This is not observed for phosphoryl transfer enzymes such as βPGM, PGK, PSP, or MEK6. Indeed, in the case of βPGM, the MgF_3^- TSA complex is far less stable than the AlF_4^- complex even when Al^{III} is stoichiometric with protein and Mg^{II} is in 500-fold molar excess.[2d] Only AlF_4^- complexes have been observed for MEK6/p38α even with Mg^{II} in a 50-fold excess over Al^{III}.[2i] By contrast, cAPK (600 μM), Mg^{II} (20 mM), and Al^{III} (1.8 mM) gives an equal population of MgF_3^- and AlF_4^- TSA solution complexes at pH 7.5, showing an apparent binding constant for the MgF_3^- complex only some 10-fold weaker than for the AlF_4^- equivalent (Figure 1b). It is essential to note that MgF_3^- has a low availability in solution and thus the intrinsic binding of these enzymes for MgF_3^- must be strong.[2c]

cAPK is thus unique in showing substantially elevated natural affinity for MgF_3^- relative to AlF_4^-. This must derive from a proportionately greater priority for the geometry (tbp versus octahedral) relative to anionic charge for cAPK than is shown by other phosphoryl transfer enzymes. In part, this can be attributed to hydrogen-bonding network changes (Figure 2). In the tbp complex, F_A forms regular hydrogen bonds with amides Ser53 in cAPK and Ser17 in SP20, while in the octahedral complex, F_A is only weakly directed at Ser53 and coordination to Ser17 is lost. In MEK6, its dual specificity role must accommodate either tyrosine or serine with comparable facility in TS complexes,[2i] so the equivalent organization of hydrogen bonds involving the substrate backbone may play a lesser role.

Notwithstanding this significant shift in prioritization of charge relative to geometry, cAPK fully adheres to the general pattern of magnesium-catalyzed kinases in obeying the CBH for an in-line transition state for transfer of the γ-phosphoryl group of ATP. The co-existence of an octahedral tetrafluoroaluminate and a tbp trifluoromagnesate transition-state-analog complex for cAPK in solution and in the solid state provides a quantitative foundation for computational analysis of the electrostatic and ligand components of transition-state stabilization in this key protein kinase.

Received: June 1, 2012
Revised: October 10, 2012
Published online: November 5, 2012

Keywords: enzyme catalysis · kinases · NMR spectroscopy · proteins · transition states

[1] G. Manning, D. B. Whyte, R. Martinez, T. Hunter, S. Sudarsanam, *Science* **2002**, *298*, 1912–1934.
[2] a) M. W. Bowler, M. J. Cliff, J. P. Waltho, G. M. Blackburn, *New J. Chem.* **2010**, *34*, 784–789; b) J. L. Griffin, M. W. Bowler, N. J. Baxter, K. N. Leigh, H. R. Dannatt, A. M. Hounslow, G. M. Blackburn, C. E. Webster, M. J. Cliff, J. P. Waltho, *Proc. Natl. Acad. Sci. USA* **2012**, *109*, 6910–6915; c) N. J. Baxter, L. F. Olguin, M. Golicnik, G. Feng, A. M. Hounslow, W. Bermel, G. M. Blackburn, F. Hollfelder, J. P. Waltho, N. H. Williams, *Proc. Natl. Acad. Sci. USA* **2006**, *103*, 14732–14737; d) N. J. Baxter, G. M. Blackburn, J. P. Marston, A. M. Hounslow, M. J. Cliff, W. Bermel, N. H. Williams, F. Hollfelder, D. E. Wemmer, J. P. Waltho, *J. Am. Chem. Soc.* **2008**, *130*, 3952–3958; e) N. J. Baxter, A. M. Hounslow, M. W. Bowler, N. H. Williams, G. M. Blackburn, J. P. Waltho, *J. Am. Chem. Soc.* **2009**, *131*, 16334–16335; f) M. Golicnik, L. F. Olguin, G. Feng, N. J. Baxter, J. P. Waltho, N. H. Williams, F. Hollfelder, *J. Am. Chem. Soc.* **2009**, *131*, 1575–1588; g) N. J. Baxter, M. W. Bowler, T. Alizadeh, M. J. Cliff, A. M. Hounslow, B. Wu, D. B. Berkowitz, N. H. Williams, G. M. Blackburn, J. P. Waltho, *Proc. Natl. Acad. Sci. USA* **2010**, *107*, 4555–4560; h) M. J. Cliff, M. W. Bowler, A. Varga, J. P. Marston, J. Szabo, A. M. Hounslow, N. J. Baxter, G. M. Blackburn, M. Vas, J. P. Waltho, *J. Am. Chem. Soc.* **2010**, *132*, 6507–6516; i) X.-X. Liu, J. P. Marston, N. J. Baxter, A. M. Hounslow, Y.-F. Zhao, G. M. Blackburn, M. J. Cliff, J. P. Waltho, *J. Am. Chem. Soc.* **2011**, *133*, 3989–3994.
[3] J. K. Lassila, J. G. Zalatan, D. Herschlag, *Annu. Rev. Biochem.* **2011**, *80*, 669–702.
[4] D. L. Graham, P. N. Lowe, G. W. Grime, M. Marsh, K. Rittinger, S. J. Smerdon, S. J. Gamblin, J. F. Eccleston, *Chem. Biol.* **2002**, *9*, 375–381.
[5] J. Y. Lee, W. Yang, *Cell* **2006**, *127*, 1349–1360.
[6] A. Wittinghofer, *Curr. Biol.* **1997**, *7*, R682–R685.
[7] a) C. Chaudhry, A. L. Horwich, A. T. Brunger, P. D. Adams, *J. Mol. Biol.* **2004**, *342*, 229–245; b) J. M. Davies, A. T. Brunger, W. I. Weis, *Structure* **2008**, *16*, 715–726.
[8] M. Klähn, E. Rosta, A. Warshel, *J. Am. Chem. Soc.* **2006**, *128*, 15310–15323.
[9] S. S. Taylor, A. P. Kornev, *Trends Biochem. Sci.* **2011**, *36*, 65–77.
[10] a) P. A. Madhusudan, N. H. Xuong, S. S. Taylor, *Nat. Struc. Biol.* **2002**, *9*, 273–277; b) Z. Q. Bao, D. M. Jacobsen, M. A. Young, *Structure* **2011**, *19*, 675–690.
[11] a) T. Langer, M. Vogtherr, B. Elshorst, M. Betz, U. Schieborr, K. Saxena, H. Schwalbe, *ChemBioChem* **2004**, *5*, 1508–1516; b) L. R. Masterson, C. Cheng, T. Yu, M. Tonelli, A. Kornev, S. S. Taylor, G. Veglia, *Nat. Chem. Biol.* **2010**, *6*, 821–828; c) L. R. Masterson, L. Shi, E. Metcalfe, J. Gao, S. S. Taylor, G. Veglia, *Proc. Natl. Acad. Sci. USA* **2011**, *108*, 6969–6974.
[12] B. E. Kemp, D. J. Graves, E. Benjamini, E. G. Krebs, *J. Biol. Chem.* **1977**, *252*, 4888–4894.
[13] R. B. Martin, *Coord. Chem. Rev.* **1996**, *149*, 23–32.
[14] P. E. Hansen, H. D. Dettman, B. D. Sykes, *J. Magn. Reson.* **1985**, *62*, 487–496.
[15] Complex generated by soaking the small molecule components into a pre-existing apoprotein crystal.
[16] J. Raingeaud, S. Gupta, J. S. Rogers, M. Dickens, J. Han, R. J. Ulevitch, R. J. Davis, *J. Biol. Chem.* **1995**, *270*, 7420–7426.

